Surface Science 621 (2014) 69–76

Contents lists available at ScienceDirect

Surface Science

journal homepage: www.elsevier.com/locate/susc

Atomic layering and misfit-induced densification at the Si(111)/In solid–liquid interface

Vedran Vonk [a,b,*], Melissa Cremers [a], Aryan de Jong [c], Stelian Pintea [c], Elias Vlieg [a]

[a] Radboud University Nijmegen, Institute for Molecules and Materials, NL-6525AJ Nijmegen, The Netherlands
[b] Deutsches Elektronen-Synchrotron (DESY), D-22607 Hamburg, Germany
[c] European Synchrotron Radiation Facility, F-38043 Grenoble, France

ARTICLE INFO

Article history:
Received 1 August 2013
Accepted 24 October 2013
Available online 9 November 2013

Keywords:
Solid–liquid interfaces
Semi-conductor metal interfaces
Surface x-ray diffraction

ABSTRACT

We report on the solid–liquid interface structure between Si(111) substrates and indium at temperatures just above its melting point. At similar metal–semiconductor interfaces, liquid density enhancements have been observed by Reichert et al. [1]. Our surface x-ray diffraction study reveals that there is pronounced layering of the liquid near the interface. The data allow for identifying both layering length scales: the interlayer distance of 2.2 Å and the decay length of approximately 15 Å. Furthermore do we find the very first layer of indium adjacent to the Si(111) to be partially laterally ordered at the substrate's hollow sites. We introduce a hard sphere packing model that can explain the experimentally observed layering distance and anisotropic order. This packing also reveals that due to the misfit between the size of the indium atoms and the periodicity of the substrate, the indium atoms can pack together closer than in the bulk liquid. These results show that the lateral interaction between the substrate and the liquid directly influences the layering distance and that the resulting packing can account for part of the previously observed enhanced densities.

1. Introduction

Solid–liquid interfaces are relevant for processes in a range of areas, including biology, physics, chemistry and engineering. The interaction between a solid and a liquid, and its emerging interface structure, is of importance for obtaining an understanding of e.g. transport properties around cells or friction and lubrication in mechanical systems. In particular, the interactions between the solid and the liquid on the nanometer scale govern nanotechnological fabrication processes which take place at these interfaces. Also growth of high quality semi-conducting devices by for example the Vapour–Liquid–Solid (VLS) method or Liquid Phase Epitaxy (LPE) takes place at solid–liquid interfaces between semiconductors and metals. In order to obtain a microscopic understanding of crystal growth at such interfaces, it is mandatory to gain a detailed picture of the interface at the atomic scale. The details of compositional changes induced by segregation and the characteristic width over which the atomic order changes from solid to liquid are important to understand the energetics and kinetics governing crystal growth. In addition, such studies will be important for identifying the combination of parameters which allow for nanoscale control over the growth.

A number of studies have been performed on (sub)monolayer liquid films [2–7] on a substrate, but in order to see the evolution to a bulk liquid thicker films have been investigated [8]. Such studies revealed several structural properties of the interfacial liquid, such as atomic layering [9], local five-fold symmetry [10] and preferential in-plane ordering of the first layer(s) [11]. Only few studies on a limited number of systems have been conducted and a complete description of the solid–liquid interface structure is still missing. The main reason is that the atomic interactions, needed for theoretical calculations, are difficult to compute and that experimentally the deeply buried interfaces are difficult to address with traditional probes. Reichert et al. [1] have investigated several semi-conductor/metal solid/liquid interfaces and made the puzzling observation of a huge densification up to 40% of the liquid near the interface. The densification extends up to 2 nm into the liquid, much larger than any screening length in the investigated metals. Nevertheless, Reichert et al. argue that the phenomenon is of electronic nature by the metal continuously feeding the semi-conductor's conduction band with electrons. The change in valence, and subsequently of the atomic radii, is thought to result in a denser packing. The same densification phenomenon, albeit less pronounced, has been observed at the Hg–Al_2O_3 interface [12]. A recent molecular dynamics study of this interface concludes that even without the assumption of electron transfer (and a corresponding shrinkage of the atoms) a densification is expected [13]. These studies raise the question to what extent the densification phenomenon applies generally to solid–liquid interfaces. Here we target this problem by studying the atomic stacking, which should comply with all the experimentally observed phenomena, such as layering, local five-fold symmetry and densification. The most important result is that the lateral interaction between the substrate and liquid can result in local densification. This phenomenon can

* Corresponding author at: Deutsches Elektronen-Synchrotron (DESY), D-22607 Hamburg, Germany. Tel.: +49 40 8998 6012; fax: +49 8998 6013.
E-mail address: vedran.vonk@desy.de (V. Vonk).

0039-6028/$ – see front matter © 2013 Elsevier B.V. All rights reserved.
http://dx.doi.org/10.1016/j.susc.2013.10.022

account for part of the previously found huge enhancements, which still can be only explained by unusually short quasi-liquid interatomic distances.

Here we report on the interface structure between liquid indium and a Si(111) substrate. The main observations are that atomic layering occurs with a very small spacing and extends up to approximately 7 layers into the liquid. Furthermore, the very first layer of the indium atoms shows in-plane order, whereby the atoms preferentially occupy hollow sites of the underlying Si(111) substrate. We also investigate how such an ordered indium layer serves as a template for further quasi-liquid metal layers. By making use of the model set out by Spaepen [14], we show how the misfit between the indium atoms' size and the substrate's in-plane lattice constant can lead to a densification compared to bulk liquid indium of the first quasi-liquid layer(s).

The remainder of this article is organized as follows. First we describe x-ray scattering from solid–liquid interfaces. This section also introduces the structural fit models used in our data analysis. Next we present the experimental data and the resulting fits. In a separate section the hard-sphere packing model is introduced, after which this model is compared with the experimental results and discussed in relation to other solid–liquid interfaces.

2. X-ray scattering from solid–liquid interfaces

Crystals show long-range atomic order whereas liquids only display short-range order. Hence, the corresponding scattering patterns, which can be calculated through Fourier transform of the real-space electron densities, are very different. At the interface between solids and liquids some of the solid's Fourier components will be transmitted to the liquid in a thin region close to the interface. By measuring the crystal truncation rods (CTRs) of the solid in contact with the liquid, it is possible to determine the degree by which the liquid orders with respect to the solid [11]. The challenge to experimentally solve the complete 3D atomic structure of a solid–liquid interface lies in the fact that the signals obtained by such diffraction techniques are relatively weak, because of the disorder, and are further obscured by the relatively high background signal from the bulk liquid scattering [15].

Atomic layering will result in a Bragglike feature on the specular CTR at a point in reciprocal space $Q = 2\pi/d$, with d the layer spacing and $Q = 4\pi\sin(\theta)/\lambda$ the momentum transfer (where θ is half the scattering angle and λ is the wavelength). Such a layering signal was found at the AuIn–InP(111) interface, giving evidence of a layering distance of 2.3 Å [16]. Densification and/or layering phenomena which appear on a length scale several times the layering distance are expected to show up at lower momentum transfer in the scattering pattern. To the best of our knowledge, so far there has been only one study attempting to reveal both length scales [12]. Those data did not show a clear Bragglike feature and the details for this system seem to be rather subtle, which might also come from the use of a miscut substrate.

In the next sections the structural model and the scattering calculation used in the data analysis are presented.

2.1. In/Si(111) scattering calculation

Fig. 1 shows schematically the atomic-scale model that is used in the data analysis.

The scattering amplitudes are calculated by summing over the individual atoms' scattering contributions:

$$F(Q) = \frac{F^{Si}(Q)}{1-e^{-iQ\cdot c}} + \sum_{j=1} \theta_j f^{In}(Q) e^{-\frac{1}{2}U_j^{//}Q_{//}^2} e^{-\frac{1}{2}U_j^{\perp}Q_{\perp}^2} e^{iQ\cdot r_j}, \quad (1)$$

with F^{Si} the bulk silicon structure factor, Q the momentum transfer, θ_j the occupancy of the j-th atom, f^{In} the indium atomic scattering factor, $U^{//}$ and U the squared mean displacement amplitudes of the atoms parallel and perpendicular to the interface and r_j the atomic positions. The first term at the right-hand-side renders the well-known CTR [17] of the Si(111) substrate. The values U for the displacements are related to the Debye–Waller parameters by $B = 8\pi^2 U$, where in the present case the physical origin of the disorder is not only temperature vibration around an average position but also the fact that the scattering object is quasi-liquid: the average atomic positions are substantially smeared out [11]. The interface introduces an anisotropy between the in-plane and out-of-plane directions. It is therefore expected that the atoms will order differently in the two directions, which can be modelled by the use of different values for $U^{//}$ and U. In particular, the CTRs with h, $k \neq 0$ also probe atoms with in-plane order. To solve the complete 3D structure of the interface both the specular and CTRs with in-plane momentum transfer are needed.

Fig. 1 shows the top view structure of the first indium layer on the Si(111) substrate surface. As discussed later on, we obtain the best fits when a single layer of indium atoms preferentially occupies Si(111) hollow sites. The next layers of indium, starting from 2, do not show any in-plane ordering and are described in the models using very large values for $U^{//}$. In this way their scattering contributes only to the (0,0) CTR and not to any having in-plane momentum transfer. The summation over indium layer 2 and further of Eq. (1) is then calculated with a specific profile describing the degree of perpendicular ordering in the near interface region: close to the interface the ordering will be higher (and the values for U lower) than further away.[1] We have also tested the so-called distorted crystal model [18], which has been successfully used to describe liquid layering in other systems. For the data obtained here this did not lead to high quality fits, mostly because that model failed to give an adequate description over the total Q-range.

The best fit results are obtained when the scattering contributions of the indium atoms quickly diminish with distance j from the interface, either by a vanishing profile for θ_j or by a diverging profile for $U_j^{\perp}$. Although the parameter θ implies the presence of atoms, it is actually the scattering strength that is probed; not all the atoms illuminated by the x-ray beam will contribute to the CTR signals. Different profiles have been tested during the data analysis and two of these, hereafter referred to as models 1 and 2, will be shown here. The purpose of presenting two models is to explore the boundary values and sensitivity of the used method towards the different structural features that are contained by the data. It also shows that different ways of parameterizing a density profile can lead to very similar solutions, by which means the significance of certain details is tested.

2.2. Model 1

In the first model, the layerwise occupancies θ_j and amplitudes $U_j^{\perp}$ from Eq. (1) are chosen to have the following form:

$$\theta_j = \theta_0 \frac{1}{2}\mathrm{erfc}\left[\left(j - j_0^{\theta}\right)/\sigma_{\theta}\right] \quad (2)$$

and

$$U_j^{\perp} = 2U^{\perp}/\mathrm{erfc}\left[\left(j - j_0^{U}/\sigma_U\right)\right], \quad (3)$$

[1] Eq. (1) includes to some extent the liquid scattering by the use of very large values for U, which would mean that the atom is completely disordered. This is, however, not a correct description of liquid scattering, of which the well-known profiles exhibit several peaks as a function of momentum transfer. It has to be emphasized that here this (bulk) liquid scattering pattern is treated as background, and as such subtracted from the raw data in order to reveal the contribution of the ordered interface region to the scattering. As a result, those atoms that are given very large values of U in the model do not contribute significantly to the CTRs as shown in Fig. 3. This is particularly true for the atoms making up the bulk liquid electron density further away from the interface. This situation is similar to the way in which x-ray reflectivity data are analyzed. Often, the derivative of the electron density $d\rho/dz$ is Fourier transformed in such models, which results in a zero contribution from constant density profiles.

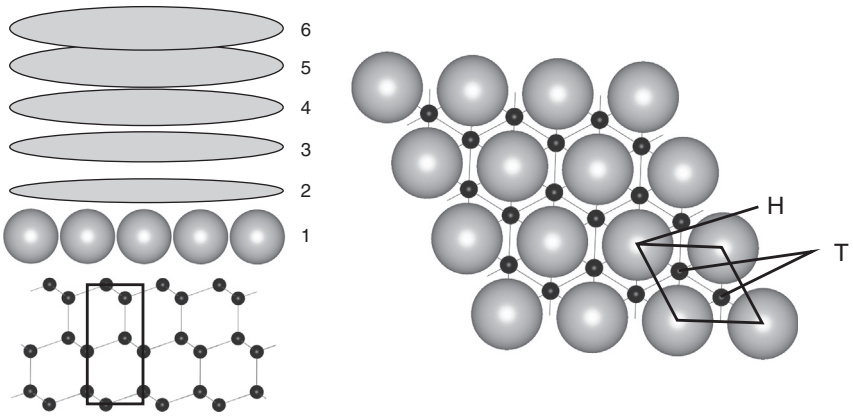

Fig. 1. Schematic of the atomic scale model used in the data analysis. (Left) Side view of the Si substrate (black) covered by In (grey), where the size of the atoms is an indication of the degree of (anisotropic) order and scales with $U^{//}$ and $U^{\perp}$. Layer 1 is partly in registry with the substrate, whereas from layer 2 onwards there is no in-plane order anymore. Layers 1–6 are indicated, although in the data analysis many more layers are included. The rectangle indicates the 6 atoms (3 bi-layers) making up the Si(111) surface unit cell. (Right) Top view showing the preferential ordering of layer 1 indium at hollow (H) sites, as compared to top (T) sites. The surface unit cell is indicated by the lozenge.

where values for σ define characteristic length scales of the corresponding parameters. The occupancies θ become essentially 0 (below the detection limit) at a distance $j = j_0^{\theta} + 2\sigma_{\theta}$ from the interface, which is interpreted to mean that there the structure has changed such that the metal's scattering does not contribute significantly to the CTRs anymore. The profile for U describes a similar decrease in indium scattering contribution, only with a different Q-dependence. Indium layer 1 is at a height z_1 above the Si substrate. The positions z_j of indium layers 2 and onwards with respect to indium layer 1 are given by:

$$z_j = (j-1)d, \quad \text{with } j=2,3,4\ldots \tag{4}$$

and with d a constant spacing between the atomic layers. In this way the positions of the indium layers are described by two independent fit parameters.

2.3. Model 2

Another way of describing the interface profile is by assuming a constant θ_j, which is a better description of the real electron density because it assumes that actual atoms are present. The values of U then determine to what extent the atoms contribute to the scattering pattern. Here, we use an exponential profile:

$$U_j^{\perp} = U^{\perp} e^{j/\sigma U}, \tag{5}$$

where σ_U is the characteristic decay length of the ordering. Furthermore, the best fit result was obtained when the positions of the atoms z_j were described by:

$$z_j = \frac{1}{2}\left(\mathrm{erf}\left(\left(j-2j_z^0\right)/\sigma_z\right)+1\right)(d_l-d)+d. \tag{6}$$

This profile describes the change from the quasi-liquid layering distance, d, in the interface's vicinity to the average distance between atoms in the bulk liquid, d_l. Since it is to be expected that the layering and ordering are closely related, the fit has been obtained using $\sigma_z = \sigma_U$ and $j_z^0 = \sigma_U$. A value of $d_l = 3.1$ Å was taken to match the nearest-neighbour distance in bulk liquid indium [19].

2.4. Density profiles

The structural models from the previous sections can also be used to calculate the out-of-plane density profile near the interface, which is commonly used to describe the quasi-liquid and its relation to bulk liquid radial distribution functions. The scattering density profile $\rho(z)$ is obtained by summing over the different layers, describing Gaussian-shaped atoms as:

$$\rho(z) = \sum_k \frac{\theta_k Z_k^a}{\sqrt{2\pi}\sigma_k} e^{-\frac{1}{2}(z-z_k)^2/\sigma_k^2} \tag{7}$$

The positions of the atoms are z_k and the atomic number Z_k^a is 14 for silicon atoms in the substrate and 49 for indium.

3. Experiment

Several thin film samples were made in the following way. Silicon wafers are cut into 10×10 mm^2 pieces and are flash-annealed in an ultra high vacuum chamber (base pressure 10^{-10} mbar). The appearance of the Si(111)(7×7) surface reconstruction, as observed by reflection high-energy electron diffraction, indicates the surfaces (for a large part) to be clean and free of oxide. After cool-down to room temperature, indium is evaporated by a Knudsen cell. Finally, the samples are capped by evaporating SiO_2 on the indium covered Si substrates in a separate deposition chamber. The In and SiO_2 thicknesses were roughly calibrated and more precisely determined using x-ray reflectivity to be 300 nm and 800 nm, respectively. In this way, thin film samples are produced of which the inert capping layer's function is twofold: protecting the interface from oxidation and preventing the metal from dewetting during liquation.

Surface x-ray diffraction experiments were carried out at beamline ID03 of the European Synchrotron Radiation Facility, France [20], using a wavelength of 0.517 Å. The samples were loaded into a small furnace, equipped with a cylindrical beryllium window, which was mounted on the diffractometer. CTR data were collected, integrated and corrected in a standard way [21], taking special care of absorption corrections necessary for the used thin film geometry.

The hexagonal Si(111) surface unit cell is related to the primitive diamond structure by: $a_s = b_s = \frac{1}{2}\sqrt{2}a_c \equiv a_0 c_s = \sqrt{3}a_c$, with a_c the cubic Si cell parameter. The direction of the reciprocal c-axis, c_s^* is along the surface normal, which is the z-direction in the surface frame. As usual, the in-plane momentum transfer components will be referred to as (h,k) and the vertical one by l.

Data were collected by a combination of rocking scans and using the so-called stationary mode [21], both of which gave the same results. Fig. 2 shows the corresponding rocking scans that were recorded at $L = 4.03$ on the (0,0) CTR and at $L = -1.8$ on the (1,0) CTR. The integrated intensities around the layering peak on the (0,0) CTR are statistically relevant ($F > 5\sigma(F)$), whereas for $L > 5$ the signals became very weak ($F \simeq \sigma(F)$). These weak points were nevertheless included in the

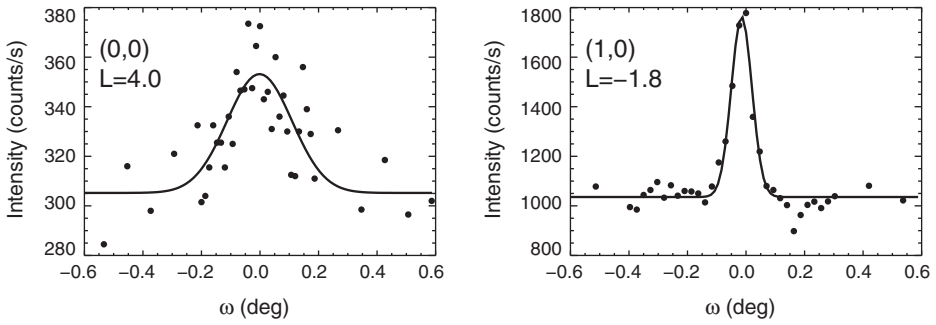

Fig. 2. Rocking scans: data points (black dots) and Gaussian fits (black lines). (Left) The point on the (0,0) CTR around $L = 4.0$ is directly related to the indium quasi-liquid layering distance. (Right) On the point on the (1,0) CTR around $L = -1.8$ s there is a contribution from in-plane ordered quasi-liquid indium.

fits, because they were found to be important upper limits and prevented diverging values for the fit parameters.

4. Results

Fig. 3 shows the (0,0) and (1,0) CTRs from the interface at 443 K, which is about 14 K above the indium melting temperature. The absence of indium powder peaks, which are observed at room temperature, shows that the metal is molten. There are three features that stand out in the measured profiles compared to those expected from bulk-terminated Si(111) in contact with a homogeneous structureless liquid: a shoulder on the high-angle side of the silicon (1,1,1) Bragg peak around $L = 4$ on the (0,0) CTR, a kink around $L = 0.2$ on the (0,0) CTR and an enhancement in intensity on the (1,0) most notably in the region between $L = -4$ and $L = 0$. These are signatures of, respectively, layering, a modified density as compared to the bulk liquid over an extended near-interface region and preferential in-plane ordering of indium. Models 1 and 2, as introduced in Section 2, are tested against the data and will be discussed hereafter. The final fit results are listed in Table 1.

The enhancement on the (1,0) CTR around $L = -2$ is best reproduced when a single layer of indium atoms is partly in registry with the substrate; more layers would result in thickness oscillations and the fit without such in-plane ordering is clearly worse, which is also reflected in the poorer fit quality having $\chi^2 = 2.3$ (using model 1). This layer 1 contains indium atoms which can reside at hollow or top sites. The best fit shows that for the largest part indium orders at hollow sites, but that a minor part can also occupy top sites. Such a mixture of co-existing preferential sites has been found previously for close-to-monolayer coverages of Pb or Sn on Ge(111) [22,4] and Bi on Cu(111) [7]. In the final fits the minor top site ordering has been discarded since it correlates strongly with the other parameters thereby showing that the information contained by the data starts to be exhausted by including such details in the model. It was also found that better fits were obtained by including a roughness parameter according to the β-model [17]. Inclusion of such a roughness parameter results in several features on the CTR profiles. In general, roughness leads to a loss of scattered intensity at the surface sensitive parts, whereas it leaves the intensities close to the Bragg peaks unaltered. Around $L = 6$ on the specular CTR there is an (apparent) increase in calculated structure factor. This is around the bulk forbidden (2,2,2) Bragg reflection, a point in reciprocal space where there are no phase differences between x-rays scattered by different layers. This point is therefore not sensitive to surface roughness, but the regions at lower and higher momentum transfer do diminish. This leads to small apparent enhancements around $L = 6$ on the (0,0) and $L = -2$ on the (1,0) CTRs. However, the region around $L = -2$ on the (1,0) CTR is the best reproduced by including both roughness and in-plane ordering; including either of the two does not result in the observed shape. This becomes clearer from fitting model 1 without including in-plane ordering of layer 1 (see Fig. 3). Although there is an apparent enhancement around $L = -2$ on the (1,0) CTR, the fit is clearly too low in that region. By including in-plane ordering of layer 1, the intensity is lifted to higher values in the whole region, as indicated by the data. The reason that one can distinguish between roughness and in-plane ordering is that all the CTR data are sensitive to roughness and therefore jointly determine the roughness parameter. The parameters describing the in-plane ordering are then determined independently.

Within fit model 2 the scattering contribution from indium atoms further away from the interface leads to pronounced oscillations in

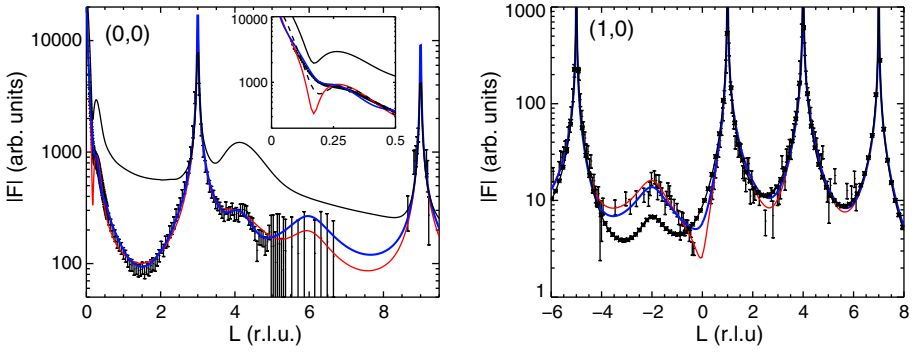

Fig. 3. Experimental CTR data and fits. (Left) Specular CTR with fits using a vanishing indium occupancy profile (model 1, blue/thick) and a constant one (model 2, red/thin), as discussed in the text. The inset shows an enlargement of the low-L range, where the dashed line is obtained by convolving the fit with the constant indium occupancy model (red) with a Gaussian of which the width complies with the x-ray beam divergence. Also shown is the calculated CTR when assuming a perfect interface having constant bulk liquidlike indium occupancy and no surface roughness (dash dot), which shows nearly the same shape as the fit models, but with an enhanced signal level. (Right) (1,0) CTR data and fits (model 1 blue/thick, model 2 red/thin). Both fits are nearly identical because only the indium atoms of layer 1 contribute to scattering with in-plane momentum transfer; the rest of the layers are assumed to have no in-plane order. Also shown is the fit when excluding in-plane ordering of layer 1, thereby revealing the CTR shape including the apparent enhancement due to surface roughness (black connected asterisks). Clearly this fit model fails to describe the data in the region $L = -4$ to $L = -0$ and the value $\chi^2 = 2.3$ is significantly worse than that obtained with model 1 ($\chi^2 = 1.3$). (For interpretation of the references to colour in this figure legend, the reader is referred to the web version of this article.)

Table 1
Optimum parameter values for the two different fit models. The parameters are defined by Eqs. (1)–(6). The subscript 1 refers to structural parameters of layer 1, where z_1 indicates the distance from layer 1 to the last layer of Si substrate atoms. The layering distance in the quasi-liquid is given by d. The β-roughness model parameters and final χ^2 values are indicated as well.

	Model 1	Model 2
First layer		
z_1(Å)	2.76(2)	2.76(1)
$U_1^{\perp}$(Å^2)	0.07(1)	0.10(1)
$U_1^{//}$(Å^2)	1.1(1)	0.76(1)
θ_{hol}	0.59(2)	0.65(1)
Quasi-liquid		
d(Å)	2.21(2)	2.12(1)
$U^{\perp}$(Å^2)	0.19(1)	0.33(1)
σ_U	13.2(3)	2.80(1)
J_U^0	−3.7(6)	
$U//$(Å^2)	6.3	6.3
θ_0	1.33(2)	0.61(1)
σ_θ	23(1)	
J_θ^0	0.0(3)	
Other		
β	0.30(1)	0.31(1)
χ^2	1.3	4.8

the low Q part, even with the quickly diverging exponential profile for U. This effect is becoming even worse when using a 'flat' profile for z_j instead of the erf-profile used now. The data do not show such pronounced oscillations, but do show a kink indicative of a length scale between 1 and 2 nm. Although the final χ^2 value for model 2 seems much worse than for model 1, for the largest part this is caused by the poorer fit of only a few data points around the low-Q kink. Such strong oscillations will be damped by causes such as sample curvature or x-ray beam divergence. In Fig. 3 the effect on the low Q range of the (0,0) CTR is shown of a convolution with a Gaussian having a width of the x-ray beam divergence. This convolution has a significant effect only on the low Q range, because for higher scattering angles the features are already much broader.

Fig. 4 shows the density profiles, calculated as described in Section 2.4, obtained from models 1 and 2. The layerwise atomic occupancies and disorder from the best fit model 1 are also shown in Fig. 4.

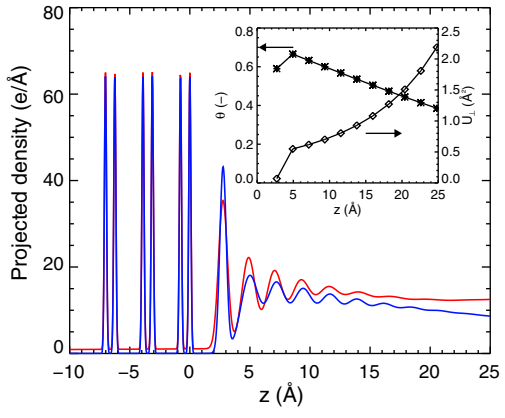

Fig. 4. Projected (scattering) density profile of the Si(111)–In interface along the surface normal direction (z), of which the origin lies at the last layer of Si substrate atoms. Shown are the profiles obtained with a vanishing indium occupancy profile (blue/lower) and a constant one (red/upper). The gradually decreasing profiles originate from the fact that atoms further away from the interface do not contribute to the scattering, as discussed in the text. The inset shows the quasi-liquid layerwise average atomic occupancies, θ (asterisks), and the out-of-plane disorder, $U\perp$ (diamonds), as obtained from model 1. (For interpretation of the references to colour in this figure legend, the reader is referred to the web version of this article.)

5. Hardsphere packing model

We will now compare the experimental structural features with a hard-sphere model, thereby focussing especially on the first two atomic layers of the quasi-liquid. The aim is to investigate by means of a relatively simple model how the atoms could stack across the interface and how this influences the layering distance, disorder and local density. By the use of this model it is possible to directly compare and interpret quantitatively some of the experimentally determined structural features. It is important to note that the goal of this description is not to disclose all the details of the quasi-liquid's structure, which involves more than just the two first layers. As a starting point we take the model by Spaepen [14], who introduced a solid–liquid interface model for a crystal in contact with its own melt. The atoms' stacking is subjected to specific rules, which are based on maximizing the number of tetrahedral configurations on the liquid side. As a result, there are three planar configurational motifs, triangular, rectangular and pentagonal, which make up a 2D layer without in-plane long-range translational order. Schematically such a layer is shown in Fig. 5.

The very first layer 1, which is in contact with the substrate, does show in-plane order, and serves as a template onto which indium layer 2 is stacked. As a first approximation we presume layer 1 to be completely preferentially ordered at substrate hollow sites, thereby forming a hexagonal close packed crystal plane. Although the ordering will not be as strong as assumed, well-defined average atomic positions of the first layer have also been found from molecular dynamics studies [23,24]. We take the indium diameter to be $d_0 = 3.14$ Å, a value which complies with bond lengths in the solid [25] as well as the nearest-neighbour distance (d_{NN}) in the liquid [19]. The distance between Si(111) hollow sites is given by the in-plane cell parameter $a_0 = 3.84$ Å. Because of the size-lattice mismatch, the atoms within layer 1 cannot touch each other. Compared to a homointerface, the atoms from layer 2 can sink deeper into layer 1, thereby filling up part of the empty space within this layer. Since the atoms in layer 1 are laterally spaced further apart so will be the atoms in layer 2, which form the previously mentioned 2D motifs without long-range order. The next layer atoms, which are placed on top of the triangles, rectangles and pentagons, can again sink deeper into layer 2. Now we define a crystal slab of thickness d_0 centred on the first disordered layer 2 and calculate the number of atoms in this slab, thereby also including partial atoms from the layers above and below. Since the coverage of rectangles, triangles and pentagons in layer 2 is equal [14], it is possible to calculate the average number of atoms in a volume $V_0 = A_0 d_0$, where A_0 is the area of the substrate surface unit cell. The calculation is done as a function of the ratio a_0/d_0 as shown in Fig. 6, which also shows the layer spacing and disorder as a function of the lattice-size-mismatch. It is found that a substantial contribution to the density is coming from top atoms in between two neighbouring pentagons, as indicated by the dashed area containing a black indium atom in Fig. 6. More top atoms have not been considered, but it is clear that these will further enhance the calculated density in layer 2.

As the atoms are laterally pulled further apart due to the lattice-size mismatch, atoms from the layers above and below can sink deeper into the crystal slab which has as a result that the density increases. This description holds as long as there are equal amounts of pentagons, triangles and rectangles. In this respect, the calculation starts to fail at a ratio a_0/d_0 close to 1.24, which is the situation where some of the top atoms 'fall through' the pentagons. If these top atoms would become part of the underlying layer, additional octahedral holes would be created, which is unfavourable for a liquid and should therefore be prevented from forming. Since the structure holds the middle between a solid and a liquid, it is therefore likely for the structure to show features from both. The In–Si(111) interface is presumed to have $d_0/a_0 = 1.23$, very close to the end of the range where the current description seems to hold. It is therefore expected to have a maximal densification within the presented hard-sphere packing.

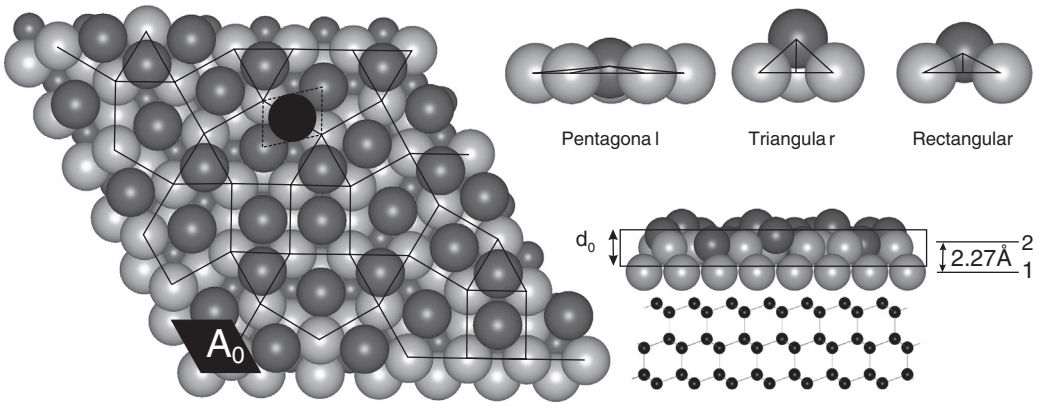

Fig. 5. Schematic of a hardsphere packing model based on Spaepen [14]. The scale is based on an indium atomic diameter of 3.14 Å and a silicon in-plane distance of 3.84 Å. (Left) Top view whereby the network of triangular, rectangular and pentagonal building blocks is indicated. Two layers of indium atoms are shown in grey. The topmost indium atoms are darker in colour and the substrate Si atoms are smaller in size. The dashed area and black indium atom indicate the space and position between two neighbouring pentagons where additional next layer atoms can be placed (see text). (Right top) Side views of the three different building blocks, whereby the position of the top atom with respect to the basal plane is illustrated. (Right bottom) Side view indicating the ordered layer 1 and disordered layer 2. The average distance between atoms in layers 1 and 2 of 2.27 Å is also given. The rectangular box of thickness d_0 is the slab in which the average density is calculated for different ratios of the substrate lattice constant (a_0) and the indium atomic diameter (d_0), see Fig. 6.

Within this hard-sphere model, the packing fraction, η, of the atoms in the quasi-liquid layer increases when the substrate pulls the atoms laterally further apart (see inset Fig. 6). The resulting packing fraction is in between the values of bulk indium ($\eta_{bulk} = 0.596$, solid and liquid have almost equal densities) and hypothetical close-packed indium ($\eta_{cp} = 0.74$). This means that in the case of liquid and solid indium there is a lot of space around the atoms and that they could draw closer together within a hard-sphere packing picture. The reason for this not happening in the bulk is that apparently the (anisotropic) bonds take up this space. At a solid–liquid interface the situation is different, since new In – Si bonds are formed. The hard-sphere packing model presented here shows that if there is preferential in plane ordering in combination with a lattice-size misfit, in principle the atoms can pack together closer. Therefore, the geometry of the hard sphere packing can also explain additional density as has been observed previously [1].

6. Discussion

In the following the present results will be discussed, thereby comparing the SXRD results and the hard-sphere packing model. Next, several other systems, which have been investigated experimentally and of which the structural details are listed in Table 2, are also compared with the hard-sphere packing model and discussed.

6.1. In–Si(111)

Several structural features of the interface between layers 1 and 2 obtained from the experimental model 1 and the theoretical hard sphere packing model are listed in Table 2. The values from the latter are obtained through straightforward geometrical calculations. Whereas the layering distance and disorder agree very well, there is a large discrepancy between the densities. The experimental data seem to indicate a huge density deficit, only approximately half of the interface is covered by indium, which is of course not physically acceptable. Both fit models 1 and 2 show a lack of density and almost equal density profiles (see Fig. 4), which is an indication that both models contain most of the important features in order to describe the data. It is known that atomic site occupancies in SXRD correlate strongly with interface roughness, a phenomenon that can take place at different length scales. In general, the β roughness model [17] used here works very well for atomic roughness. The fact that the occupancies remain far too low, even though roughness has been included, indicates that some other non-ideal interface property is present. Some possibilities are the following: 1) Patches of oxide islands remained on the Si(111) surface after flashing. Rough oxide islands would result in a locally different layering and only the strong layering on the clean parts of the substrate would show up in the scattering. 2) During the flashing of the Si(111) substrate some facetting might already have started [26]. Such long length-scale surface undulations would be detrimental to the indium layering. 3) The thin Si wafers could be bent, which results in a loss of scattered intensity [27]. 4) During deposition of the capping layer, part of the metal starts to dewet already, resulting in a wormlike network and partial substrate coverage.

The fact that RHEED of the flashed surfaces clearly showed a Si(111)(7 × 7) reconstruction is an indication that at least part of the surface was clean and well ordered. It could be that this was only the case for about half of the total surface area. Also the fact that we see a

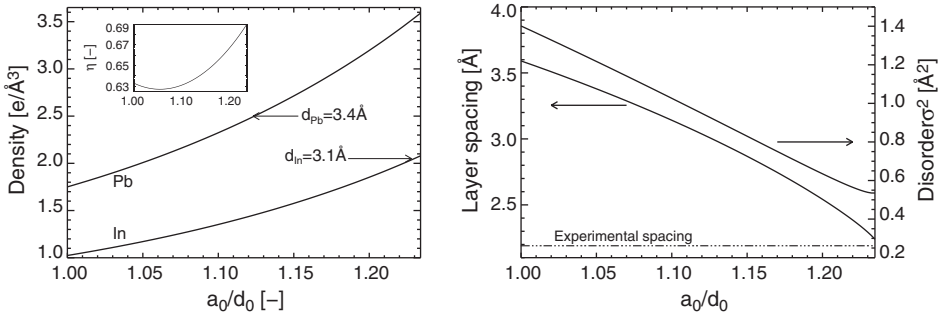

Fig. 6. Structural parameters of the hard-sphere packing model calculated as a function of the ratio between the substrate's hexagonal in-plane lattice parameter (a_0) and the liquid's atomic diameter (d_0). (Left) Indium (Z = 49) and lead (Z = 82) electron densities within a slab centred on the first disordered layer, as drawn in Fig. 5. The arrows indicate the densities expected for atomic diameters which comply with the liquid nearest-neighbour distances. The inset shows the packing fraction η as a function of the misfit ratio. (Right) Spacing between first and second indium layer and the disorder in layer 2 as explained in the text. Also shown is the layer spacing obtained from experiment (dash–dot).

Table 2
Comparison between structural parameters obtained from the present study (SXRD), the hard sphere packing model (HS), several other systems and bulk liquid indium. Listed are the following parameters, as far as they could be determined: the layering distance d, the variance σ^2 (or equivalently the atomic disorder U) of the atoms in layer 2 (the first in-plane disordered layer), the local electron/scattering density ρ and its ratio with the bulk liquid density (ρ^{liq}_{bulk}), the bulk solid density (ρ^{sol}_{bulk}) and the (hypothetical maximum) close-packed density (ρ_{cp}). Values for bulk liquid indium are determined from Ocken et al. [19] in the following way. The value for $d = \sqrt{3/4}d_{NN}$, with $d_{NN} = 3.14$ Å the nearest-neighbour distance, would be expected for cp-like stacking [32]. The value for σ^2 is determined from the width of the first maximum of the radial distribution function.

	In–Si(111)		Hg–Al_2O_3(0001)	In–Si(001)	Pb–Si(111)	Pb–Si(001)	InAu–InP(111)	Liquid In
	SXRD	HS	Ref. [12]	Ref. [1]	Ref. [1]	Ref. [1]	Ref. [16]	
d(Å)	2.21(2)	2.27	2.66				2.32(4)	2.72
σ^2(Å^2)	0.55(6)	0.5	1.3				0.4(1)	0.1
ρ(e/Å^3)	1.15(6)	2.1	3.6	2.6	3.0	3.2	1.9	1.79
ρ/ρ^{liq}_{bulk}	0.64(3)	1.2	1.10(5)	1.4	1.2	1.3	0.6	1.00
ρ/ρ^{sol}_{bulk}	0.61(3)	1.2	1.04(5)	1.4	1.1	1.2	0.6	0.96
ρ/ρ_{cp}	0.51(3)	0.95	0.9	1.2	1.1	1.2	0.5	0.8
d_0/a_0	1.23	1.23	1.5	1.23	1.1	1.1	1.4	

clear layering peak in the data indicates that at least part of the interface is ideal. Calculation of the scattering by an interface with much larger values for the indium occupancies (Fig. 3) shows that the position of the layering peak and overall CTR shape do not change significantly, but merely that everywhere a much higher intensity would occur. The occupancies for this simulation have been chosen such that they correspond to the average number of atoms on a plane through the bulk liquid. Furthermore these calculations have been performed without including any roughness thereby not showing the enhancement around $Q = 4$ Å^{-1} on the (0,0) CTR. X-ray reflectivity data taken from other samples show densities much closer to bulk indium values (and some also enhancement) [28], which corroborates the earlier found density enhancements [1,12,13]. Therefore, it seems justified to treat this interface as being ideal but only on about half the total interface area.

We rule out the possibility of enhanced interface roughness due to dissolution of silicon. From the Si–In binary phase diagram [29], it can be estimated that around 450 K less than 1 monolayer of Si should dissolve in the total indium thin film volume. This would provide enough atom mobility for the Si(111) surface to retain a flat (1×1) structure. From a thermodynamic point of view, an equilibrium would be expected between a flat (111) surface, which is known to have the lowest surface energy, and a liquid in which some Si is dissolved. It is also expected that the relatively large strain energy associated with the (7×7) reconstruction can be relieved upon interaction with the liquid. Submonolayer coverages of In on Si(111) in vacuum lead to a whole range of reconstructions [30], indicating that such surface reconstructions can fairly easily change. In the case of the buried Pb–Si(111) interface it has been shown that the (7×7) reconstruction transforms completely to (1×1) at temperatures below the melting point of Pb [31], which also confirms that a buried Si(111) interface is not reconstructed.

6.2. Other solid–liquid interfaces

Compared to In, a different situation arises at the Pb–Si(111) interface, for which the calculated density of layer 2 within the hard-sphere packing model results in a value of 2.5 e/Å^3, the same as bulk liquid lead[2] (see Fig. 6). In order to arrive at the experimentally found density of 3.0 e/Å^3 with the Si(111) interface [1], the Pb atomic diameter should be 3.25 Å, which is about 5% smaller. Such an average bond length would be expected for mixed metallic and covalent bonds, of which the latter are 2.92 Å [33]. Indeed, Pb coverages around a monolayer on Si(111) have shown to form structures exhibiting Pb–Pb distances as small as 3.0 Å [34], pointing towards a covalent bond character. This can be understood crudely by considering that with the transition of a covalent solid to a metallic liquid the interface may consist of a mixture of such bonds. Since it can be ruled out that Si will be present in large amounts (due to the low solubility), it leaves the Pb atoms to adjust to the change in bond nature, which also implies a drastic change in the electronic valence structure within the quasi-liquid region.

From the values listed in Table 2 it may be concluded that a 4-fold symmetric substrate leads to an even denser quasi-liquid packing than at a hexagonal one. Although the lattice-size misfit for the Si(001) surface is the same as for the Si(111) ($a_0 = \frac{1}{2}\sqrt{2}a_c$ in both cases), the geometry of quasi-liquid atomic structures is expected to be completely different. Indeed, for the Pb–Si(001) interface, it has been suggested that the dominant structural motif is a pentagon [10], the shape of which is regular in contrast to the pentagon considered for the (111) surface. Also in the case of a regular pentagon, the local density can increase when the basal atoms are pulled apart and the top atom sinks in deeper. Further detailed comparison with a (001) surface is hampered, since it remains unclear how to construct a space-filling atomic layer consisting of such regular pentagons and possible other motifs.

Clearly, the present hard sphere packing model cannot explain densities which are above those of a close-packed system, as in the case of Pb. This can indeed only be understood if the average distance between the atoms reduces below expected values for the liquid metal, i.e. when the atomic size reduces. But the stacking does show that by pulling atoms apart laterally, the available space can be taken up by other atoms, thereby increasing the local packing fraction. In a first order approximation this is understood from the fact that the local 'unit cell' volume increases linearly with the lateral expansion, whereas the additional partial atomic volume increases to the third power with distance. In effect, a quadratic behaviour for the local packing fraction as a function of d_0/a_0 remains, as can be seen in the inset of Fig. 6. This is true more generally and therefore can account for at least part of density enhancement at solid–liquid interfaces.

The small layering distance close to 2.2 Å found here compares rather well with the value of 2.3 Å found for the AuIn–InP(111) interface [16]. Also the atomic disorder is similar for both systems. Comparison with bulk AuIn liquid density, as shown in Table 2, is made by taking the weighted average of the densities of pure In and Au. The density of the solid is calculated from the Au_3In_2 crystal structure [35]. The close packed density (ρ_{cp}) and the value for d_0/a_0 are calculated assuming an atomic diameter of gold of 2.85 Å [36] and taking the weighted average with the values obtained for In. It is not straightforward to interpret the results in terms of the same hard-sphere packing model as presented here. First, the lattice size mismatch d_0/a_0 is outside the range of where the present hard sphere geometry seems to hold and therefore the structure will look different from the one presented here. Second, due to the mixture of In and Au and possible preferential segregation, the alloy is a more complex system. Also in the case of the InAu–InP(111) interface, the layering distance is significantly smaller than the value expected for a close packed stacking, which again can be explained by lateral ordering in combination with a substrate–liquid misfit.

A final remark needs to be made when comparing the densities of the AuIn–InP(111) and the In–Si(111) interfaces. Also there the estimated

[2] Using an atomic diameter of 3.4 Å, taken from the nearest neighbour distance in bulk liquid lead [37]. This is slightly smaller than the atomic diameter of 3.5 Å, which occurs in solid Pb and which would result in a slightly lower calculated quasi-liquid density.

density, obtained from experiments on similar capped thin film samples, is about half of what would be expected. There are two explanations for the similar low densities. The first one would be that the sample preparation and intrinsic properties of capped thin films on wafers, as discussed previously, are the cause for the low (scattering) densities. A second explanation would be that there is a substantial amount of atoms within the quasi-liquid volume which is much more disordered than those participating in the layering. As discussed in Section 2.1, diffraction techniques at relatively high momentum transfer ($Q > 2$ Å^{-1}) rely on order and therefore such disordered atoms remain 'invisible'. Although the absolute densities remain unclear, both experiments revealed layering peaks from which a layering distance is determined.

It would require more sophisticated models, including the details of the interactions, to disclose more details of the quasi-liquid atomic structure. For example, the agreement between experiment [12] and theory [13] on the Hg–Al_2O_3 interface, whereby a layering distance of about 2.7 Å is found, is very good. It is to be expected that each heterointerface will have its own quasi-liquid structure, which is to a large extent determined by the very first layer of ordered atoms. This will result in different values for the near-interface densification, and possibly also depletion. Indeed, different densities have been found for Pb–Si(111) and Pb–Si(100) [1], two interfaces for which different quasi-liquid structures are expected. From this point of view it is not surprising that the layering distance found here is significantly different from the value of 2.69 Å obtained at the liquid In/vacuum interface [32]. It is expected that the relatively simple hard sphere packing model based on the one of Spaepen [14] will be a good description for well-matched solid–liquid systems. This is mostly because it is based on homointerfaces. Except for the density, we find good agreement between experiment and the hard sphere stacking model, which shows that some of the quasi-liquid's structural features can be described by such a simple model and it is to be expected that also other solid–liquid interfaces could behave similarly. It is unclear for the moment how subsequent layers will stack in order to comply with the pronounced layering up to 7 layers. Hard-sphere stacking neglects long-range interactions, which are undoubtedly also present.

7. Summary and conclusions

We have obtained surface sensitive crystallographic data on the solid–liquid interface between Si(111) substrates and indium just above its melting point. The indium near the interface forms a quasi-liquid, which is evidenced by layering and in-plane ordering. The data show a clear layering peak, of which the position corresponds to a layering distance of about 2.2 Å. The (0,0) CTR exhibits a kink in its low Q range, indicative for the layering to persist for about 6–7 layers. Analysis of the (1,0) CTR, which probes in-plane order, shows that the indium layer closest to the substrate preferentially orders at hollow sites.

The experimental results together with the earlier reported local five-fold symmetry of the quasi-liquid [10] are ingredients for a hard-sphere packing model based on the one by Spaepen [14]. The very first partially ordered indium layer serves as a template onto which further quasi-liquid layers are stacked. These layers consist of planar motifs of triangular, rectangular or pentagonal shape, which fill up 2D space but lack long-range translational order. The disorder and layering distance found in the hard-sphere packing model are in excellent agreement with the best model fit to the experimental data. For the In/Si(111) interface, it is shown that the hard sphere packing results in an enhanced density in the first disordered layer. The packing depends on the mismatch between the size of the metal atoms and the periodicity of the substrate and increases with increasing mismatch. A similar comparison for the Pb/Si(111) interface shows no enhanced density, which was observed experimentally [1] and is thought to result from a shrinkage of the metal atoms near the interface. Also within the hard sphere packing model the Pb atomic diameter should be about 5% smaller than the nearest-neighbour distance in the bulk liquid. This also points towards a modified electronic structure in the quasi-liquid, whereby the bond character is possibly changed to be more covalent.

A hard sphere packing model, including local in-plane five-fold symmetry, is in very good agreement with the layering distance and disorder found from our SXRD measurements. The present results show how the lattice-size mismatch can lead to a layering distance much smaller than $\sqrt{3/4}d_0$, the distance expected for a close-packed structure. In addition, this model shows that the density enhancement can be partially attributed to the lattice-size mismatch between the substrate and liquid. Although the experimental data do not show a similar density enhancement, most likely due to a non-ideal interface, it has been observed previously, both in experiments [1,12] and theory [13] and now can also be explained by a simple geometrical model. Although the lattice-size mismatch cannot account for all the enhanced densities found in different solid–liquid interfaces, it may play an important role in the geometric structure and atomic packing at solid–liquid interfaces.

Acknowledgement

The authors would like to thank the ID03 staff of the ESRF and the Netherlands Organization for Scientific Research (NWO) for support through a VENI grant.

References

[1] H. Reichert, M. Denk, J. Okasinski, V. Honkimäki, H. Dosch, Phys. Rev. Lett. 98 (2007) 116101(URL http://link.aps.org/doi/10.1103/PhysRevLett.98.116101).
[2] In: X.Y. Liu, J.J. Deoreo (Eds.), Nanoscale Structure and Assembly at Solid–Fluid Interfaces, Kluwer, 2004.
[3] F. Grey, R. Feidenhansl, J.S. Pedersen, M. Nielsen, R.L. Johnson, Phys. Rev. B 41 (1990) 9519.
[4] M.F. Reedijk, J. Arsić, F.K. deheije, M.T. McBride, K.F. Peters, E. Vlieg, Phys. Rev. B 64 (2001) 033403.
[5] M.F. Reedijk, J. Arsić, D. Kaminski, P. Poodt, H. Knops, P. Serrano, G.R. Castro, E. Vlieg, Phys. Rev. B 67 (2003) 165423.
[6] M.F. Reedijk, J. Arsić, D. Kaminski, P. Poodt, J.W.M. van Kessel, W.J. Szweryn, H. Knops, E. Vlieg, Phys. Rev. Lett. 90 (2003) 056104.
[7] D. Kaminski, P. Poodt, E. Aret, N. Radenović, E. Vlieg, Phys. Rev. Lett. 96 (2006) 056102.
[8] P. Fenter, N.C. Sturchio, Prog. Surf. Sci. 77 (2004) 171.
[9] W.J. Huisman, J.F. Peters, M.J. Zwanenburg, S.A. de Vries, T.E. Derry, D. Abernathy, J.F. van der Veen, Nature 390 (1997) 379.
[10] H. Reichert, O. Klein, H. Dosch, M. Denk, V. Honkimäki, T. Lippmann, G. Reiter, Nature 408 (2000) 839.
[11] M.F. Reedijk, J. Arsić, F.F.A. Hollander, S.A. de Vries, E. Vlieg, Phys. Rev. Lett. 90 (2003) 066103.
[12] L. Tamam, D. Pontoni, T. Hofmann, B.M. Ocko, H. Reichert, M. Deutsch, J. Phys. Chem. Lett. 1 (2010) 1041.
[13] M. Zhao, S.A. Rice, J. Phys. Chem. A 115 (2010) 3859.
[14] F. Spaepen, Acta Metall. 23 (1975) 729.
[15] W.D. Kaplan, Y. Kauffmann, Annu. Rev. Mater. 36 (2006) 1.
[16] R.E. Algra, V. Vonk, D. Wermeille, W.J. Szweryn, M.A. Verheijen, W.J.P. van Enckevort, A.A.C. Bode, W. Noorduin, E. Tancini, A.E.F. deong, et al., Nano Lett. 11 (44) (2011).
[17] I.K. Robinson, Phys. Rev. B 33 (1986) 38303836.
[18] O.M. Magnussen, B.M. Ocko, M.J. Regan, K. Penanen, P.S. Pershan, M. Deutsch, Phys. Rev. Lett. 74 (1995) 4444.
[19] H. Ocken, N.J. Wagner, Phys. Rev. 149 (1966) 122.
[20] O. Balmes, R. van Rijn, D. Wermeille, A. Resta, L. Petit, H. Isern, T. Dufrane, R. Felici, Catal. Today 145 (2009) 220.
[21] E. Vlieg, J. Appl. Crystallogr. 30 (1997) 532.
[22] S. de Vries, P. Goedtkindt, P. Steadman, E. Vlieg, Phys. Rev. B 59 (1999) 13301.
[23] M. Heni, H. Löwen, Phys. Rev. E. 65 (2002) 021501.
[24] A. Hashibon, J. Adler, M.W. Finnis, W.D. Kaplan, Interf. Sci. 9 (2001) 175.
[25] J. Slater, J. Chem. Phys. 39 (1964) 3199.
[26] J.-K. Zuo, R.A. Harper, G.-C. Wang, Appl. Phys. Lett. 51 (1987) 250.
[27] M.J. Regan, P. Pershan, O.M. Magnussen, B.M. Ocko, M. Deutsch, L.E. Berman, Phys. Rev. B 55 (1997) 15874.
[28] V. Vonk, et al., 2013. (in preparation).
[29] C.D. Thurmond, M. Kowalchik, Bell. Syst. Tech. J. 39 (1960) 169.
[30] M. Kawaji, S. Baba, A. Binbara, Appl. Phys. Lett. 34 (1979) 748.
[31] C.A. Lucas, D. Loretto, Surf. Sci. 344 (1995) L1219.
[32] H. Tostmann, E. DiMasi, P. Pershan, B.M. Ocko, O.G. Shpyrko, M. Deutsch, Phys. Rev. B 59 (1999) 783.
[33] B. Cordero, V. Gómez, A. Platero-Plats, M. Revés, J. Echeverría, E. Cremades, F. Barragán, S. Alvarez, Dalton Trans. 21 (2008) 2832.
[34] C. Kumpf, O. Bunk, Z. J. H., M.M. Nielsen, M. Nielsen, J. R. L., R. Feidenhans'l, Surf. Sci. 448 (L213) (2000).
[35] K. Schubert, H. Breimer, R. Gohle, Z. Metallkd. 50 (1959) 146.
[36] J. Wilson, Metall. Rev. 10 (1965) 381.
[37] R. Kaplow, S. Strong, B.L. Averbach, Phys. Rev. 138 (1965) A1336.